Cooperation and the social brain hypothesis in primate social networks

Neil G. MacLaren¹, Lingqi Meng^{1,†}, Melissa Collier², and Naoki Masuda^{1,3,4,*}

¹Department of Mathematics, State University of New York at Buffalo, NY 14260-2900, USA

²Department of Biology, Georgetown University, DC 20057, USA

³Institute for Artificial Intelligence and Data Science,

University at Buffalo, State University of New York at Buffalo, USA

⁴Center for Computational Social Science, Kobe University, Kobe, 657-8501, Japan

†Present address: Science for Life Laboratory,

KTH - Royal Institute of Technology, Stockholm, SE-17121 Sweden and

*naokimas@buffalo.edu

(Dated: December 24, 2023)

The social brain hypothesis posits that species with larger brains tend to have greater social complexity. Various lines of empirical evidence have supported the social brain hypothesis, including evidence from the structure of social networks. Cooperation is a key component of group living, particularly among primates, and theoretical research has shown that particular structures of social networks foster cooperation more easily than others. Therefore, we hypothesized that species with a relatively large brain size tend to form social networks that better enable cooperation. In the present study, we combine data on brain size and social networks with theory on the evolution of cooperation on networks to test this hypothesis in non-human primates. We have found a positive effect of brain size on cooperation in social networks even after controlling for the effect of other structural properties of networks that are known to promote cooperation.

I. INTRODUCTION

The social brain hypothesis states that, among primates, brain size is positively associated with social complexity [1]. Group size, in terms of the number of individuals, is one aspect of social complexity [2]. Studies have found a positive association between brain size and the typical sizes of defined social units [1, 3] as well as more focused subgroups, such as the number of regular social contacts an individual maintains [4–7]. However, some studies have found stronger relationships between brain size and other behaviors, such as diet [8], or found the relationship between brain size and group size to be relatively weak [9] or inconsistent across data sets [10].

Although group size is the most studied potential correlate of brain size in the social brain hypothesis literature, it is not the only one [11]. Patterns of behavior between individuals in differentiated pairwise interactions can also be thought of as an important component of social complexity [2, 11, 12]. Such pairwise interactions can be represented as social networks. Network science is a common tool for studying complex systems, and researchers have investigated several network indices in relation to the social brain hypothesis. Examples include the number of connections an individual maintains (also known as the node's degree) [4–6], the number of different types of connections [5], the number of individuals in a subgroup who can connect to each other by a sequence of edges (i.e., the size of strongly connected components) [4], the number of connections normalized by the number of individuals (called the network density) [13], and more sophisticated measures of network structure [13, 14]. The results of all of these network-based studies are largely consistent with the social brain hypothesis.

Social networks have both benefits and costs that make them relevant to the evolution of sociality. The structure of animal social networks has been suggested to affect, for example, the speed
of diffusion of information, mating behavior, predator avoidance, communication efficiency, and
group movement [14–17]. On the other hand, network structure determines disease transmission
potential and epidemic outcomes in populations, because a pathogen can only spread if the relevant
form of contact exists between two individuals. Networks with high degree heterogeneity (i.e. high
variation in the number of contacts among individuals) have increased transmission potential due
to the presence of superspreaders which cause rapid, explosive outbreaks of disease in a population [18]. Animal social networks that we observe today may therefore be a result of evolutionary
processes in which more advantageous network structures have proliferated at the expense of less
advantageous structures under restrictions imposed by the environment and trade-offs between
different objectives.

One function for which social networks are particularly relevant is cooperation. Individuals of various animal species cooperate with each other, even cooperating with non-kin and in social dilemma situations in which non-cooperation is more lucrative than cooperation [19–25] (but see Refs. [22, 26, 27], which point out that empirical evidence of cooperation in animal groups remains relatively scarce). Although cooperation under social dilemmas is an evolutionary puzzle, theoretical research has suggested various mechanisms enabling cooperation, such as direct reciprocity (i.e., repeated interaction) and indirect reciprocity (specifically, reputation-based mechanisms) [28, 29]. Signaling, including symbolic communication, has been proposed as another mechanism that can enable cooperation [30], and recent theory has suggested that structured populations may facilitate the spread of cooperation in the presence of symbolic communication when compared to well-mixed populations [31]. The structure of social networks is itself one mechanism that may promote co-

operation, a concept known as network reciprocity [29, 32–35]. Specifically, a relatively small node degree (i.e., the number of neighboring individuals per individual) [36, 37] and heterogeneity among individuals in the network in terms of the degree [38, 39] can both promote cooperation compared to well-mixed populations depending on the assumptions underlying the evolutionary process models. In addition, it has long been known that clustering of the network (i.e., abundance of short cycles such as triangles and squares) promotes cooperation, which is often referred to as spatial reciprocity [29, 40, 41].

The purpose of the present study is to investigate the link between the social brain hypothesis and cooperation in social networks. While cooperation occurs in various animal taxa [21, 23], here we focus on non-human primates because both brain size and social network data are available for many primate species. Recently developed mathematical theory enables us to quantify the extent to which a network itself supports the spread of cooperation [37]. We use this theory and test whether species with larger brains form social networks that foster cooperation to a greater extent than networks for other species.

Specifically, using game theory and the properties of random walks on networks, Allen et al. 80 [37] derived an expression which predicts, for an arbitrary weighted, undirected network, how much 81 larger the benefit b of cooperating must be, when compared to its cost c, in order to favor the spread 82 of cooperation. The theory by Allen and colleagues relies on a death-birth process which, given an 83 invading cooperator and assuming no mutation, leads to fixation of either cooperation or defection (Fig. 1; see the Materials and methods section for details). For a given network, cooperation fixates 85 with a higher probability when b/c is larger in general. In particular, cooperation fixates with a probability larger than a baseline probability when b/c is larger than a threshold value, denoted $(b/c)^*$, and the $(b/c)^*$ value depends on the network structure (see the Materials and methods section for mathematical details). Because a small $(b/c)^*$ value implies that cooperation fixates 89 relatively easily for a relatively small value of b/c, networks with a small $(b/c)^*$ value favor the spread of cooperation. Our hypothesis is that nonhuman primate species with larger neocortex 91 ratios are associated with social networks that have lower $(b/c)^*$ values.

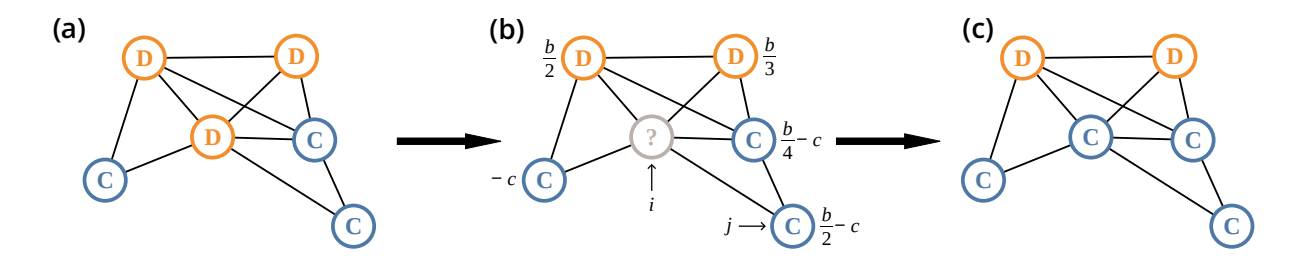


FIG. 1. A single round of the death-birth process with selection on birth. (a) Each player gains an averaged payoff by interacting with all its neighbors. We denote cooperator and defector by C and D, respectively. (b) We select a node to be updated uniformly at random. In our example we choose the node denoted by i. Then, one of i's neighbors, denoted by j, whose payoff value is shown, will replace i. We select as j each neighbor of i with probability proportional to its expected payoff; the probability to select this j is given by $[1 + \eta(b/2 - c)]/[1 + \eta(-c) + 1 + \eta(b/2) + 1 + \eta(b/3) + 1 + \eta(b/4 - c) + 1 + \eta(b/2 - c)] = [12 + 6\eta(b-2c)]/[60 + \eta(19b-36c)]$, where $\eta \ll 1$ denotes the selection strength, b denotes the benefit from cooperating, and c denotes the cost of cooperating. (c) In this example, j is a cooperator and replaces the defector on the ith node.

II. MATERIALS AND METHODS

93

94

97

98

99

100

101

A. Evolutionary game dynamics and the derivation of $(b/c)^*$

In this section, we explain the derivation of $(b/c)^*$ for any given network under the weak selection limit, following [37].

1. Networks and discrete-time random walk

We assume connected and undirected networks with N nodes. For each pair of nodes $i, j \in \{1, ..., N\}$, we denote the edge weight by $w_{ij} \geq 0$. We set $w_{ij} = 0$ if there is no edge (i, j). We allow self-loops, i.e., the case of $w_{ii} > 0$ [37]. The weighted degree of node i, also referred to as node strength, is given by $s_i = \sum_{j=1}^{N} w_{ij}$.

We start with explaining discrete-time random walks on networks because they are necessary for describing both the evolutionary game dynamics and the derivation of $(b/c)^*$. By definition, a discrete-time random walk on the network is simple if the walker located on the *i*th node moves to any *j*th node in a single time step with probability proportional to w_{ij} , i.e., with probability $p_{ij} = w_{ij}/s_i$. The transition probability matrix $P = (p_{ij})$ of the simple random walk is given by $P = D^{-1}W$, where $D = \text{diag}(s_1, \ldots, s_N)$, i.e., the diagonal matrix whose diagonal entries are equal to s_1, s_2, \ldots, s_N , and $W = (w_{ij})$ with $i, j \in \{1, \ldots, N\}$ is the weighted adjacency matrix.

Let $\pi = (\pi_1, ..., \pi_N)$ be the stationary probability vector of the random walk with transition probability matrix P. Vector π is the solution of $\pi P = \pi$ satisfying $\sum_{i=1}^{N} \pi_i = N$. It holds true for undirected networks that [42, 43]

$$\pi_i = \frac{s_i}{\sum_{\ell=1}^N s_\ell}, \quad i \in \{1, \dots, N\}.$$
(1)

2. Gift-giving game and evolutionary dynamics under the death-birth updating rule

We use the gift-giving game, also called the donation game, which is a subtype of the prisoner's 113 dilemma game. In the gift-giving game, which is a two-player game, one player, called the donor, 114 decides whether or not to pay a cost c > 0. If the donor pays c, which we refer to as cooperation, 115 then the other player, called the recipient, receives benefit b, which we assume to be larger than 116 c. If the donor decides not to pay c, which we refer to as defection, then the donor does not lose 117 anything, and the recipient does not gain anything. We assume that each player plays the game 118 with each neighbor once as donor and another time as recipient in a single round of evolutionary 119 dynamics. Then, the payoff matrix of the gift-giving game between a pair of players is given by 120

$$\begin{array}{ccc}
C & D \\
C & b - c & -c \\
D & b & 0
\end{array},$$
(2)

where C and D represent cooperation and defection, respectively, and the payoff values represent those for the row player.

We set $x_i = 0$ or $x_i = 1$ when the *i*th player is defector or cooperator, respectively. Then, the state of the entire network is specified by a binary vector $\mathbf{x} = (x_1, \dots, x_N) \in \{0, 1\}^N$. The payoff of the *i*th node averaged over all its neighbors is given by

$$f_i(\boldsymbol{x}) = -cx_i + b\sum_{j=1}^N p_{ij}x_j.$$
(3)

We set the reproductive rate of node i in state $oldsymbol{x}$ by

112

$$R_i(\mathbf{x}) = 1 + \eta f_i(\mathbf{x}),\tag{4}$$

where $\eta \ (\geq 0)$ represents the strength of natural selection. When $\eta \to 0$, the payoff, $f_i(\boldsymbol{x})$ only weakly impacts the selection, which is called the weak selection regime. A justification of weak selection is that, in reality, many different factors may contribute to the overall fitness of an individual, and the prisoner's dilemma game may be just one such contributor [36, 37].

We assume evolutionary dynamics of the gift-giving game driven by the death-birth process with selection on birth [36, 37]. By definition, we first select a node to be updated (i.e., die), denoted by i, uniformly at random. Second, we select one of the neighbors of the ith node, denoted by j, for reproduction (i.e., give birth), with the probability proportional to $w_{ij}R_j(x)$. Third, i copies the type (i.e., defection or cooperation) of j. These three steps constitute a single round of the evolutionary dynamics; see Fig. 1 for a schematic.

3. Fixation probability for cooperation and the expression of $(b/c)^*$

Because we omitted mutation, the death-birth process in any finite network eventually terminates in the state in which all individuals are uniformly cooperators or defectors. We call these
final states fixation of cooperation or defection. According to a standard convention, we assume
that the initial state contains one cooperator node and N-1 defector nodes and that each node
is the unique initial cooperator with the equal probability 1/N. We denote by $\rho_{\rm C}$ the probability
that cooperation fixates. Defection fixates with probability $1-\rho_{\rm C}$. We say that natural selection
favors cooperation if $\rho_{\rm C} > 1/N$ [36, 37, 44, 45].

Allen et al. showed that [37]

$$\rho_{\rm C} = \frac{1}{N} + \frac{\eta}{2N} \left[-c\tau_2 + b(\tau_3 - \tau_1) \right] + O(\eta^2),\tag{5}$$

146 where

145

137

$$\tau_k = \sum_{i=1}^{N} \sum_{j=1}^{N} \pi_i p_{ij}^{(k)} t_{ij}, \tag{6}$$

 $p_{ij}^{(k)}$ is the (i,j)th entry of matrix P^k , which implies that $p_{ij}^{(1)}=p_{ij}$, and

$$t_{ij} = \begin{cases} 0 & \text{if } i = j, \\ 1 + \frac{1}{2} \sum_{k=1}^{N} (p_{ik} t_{jk} + p_{jk} t_{ik}) & \text{otherwise.} \end{cases}$$
 (7)

Equation (7) implies that $t_{ij} = t_{ji}$ is the mean coalescence time of two random walkers when one walker is initially located at the *i*th node and the other walker is initially located at the *j*th node. Note that $p_{ij}^{(k)}$ is the *k*-step transition probability of the random walk from the *i*th to the *j*th node. Therefore, τ_k is the expected value of t_{ij} when *j* is the node at which the random walker arrives after *k* steps starting at the *i*th node under the stationary distribution [37]. Equation (5) implies that the natural selection favors cooperation (i.e., $\rho_{\rm C} > 1/N$) under weak selection if and only if

$$\left(\frac{b}{c}\right) > \left(\frac{b}{c}\right)^* \equiv \frac{\tau_2}{\tau_3 - \tau_1}.\tag{8}$$

It should be noted that the right-hand side of Eq. (8) only depends on the adjacency matrix of the network, W. Therefore, the network structure determines whether and how much natural selection favors cooperation in the present model. Note that $(b/c)^*$ is a threshold value: cooperation is predicted to fixate with a probability larger than 1/N when the ratio of benefit b to cost c of a particular cooperative behavior is larger than $(b/c)^*$. Thus, cooperation spreads more easily on networks with lower $(b/c)^*$.

We calculated $(b/c)^*$ for each network using our in-house code in Python 3.10, which implements the procedures described in [37]; the code is available at https://github.com/ngmaclaren/cooperationthreshold.

B. Data

The data for this study come from the Animal Social Network Repository (ASNR) [46, 47]. The ASNR contains 770 non-human social networks from eight animal classes and 69 species. For each network in this data set, nodes represent an individual animal. Edges represent a specific type of contact between two animals, such as grooming in primates and trophallaxis in ants, as well as more general contact such as group membership and spatial proximity.

There are 114 non-human primate social networks in the ASNR, including 60 grooming networks, 31 spatial proximity networks, 10 mating networks, and 13 networks with other contact types. Most sampled populations are free-ranging (84), with some captive (18) and some semi-freeranging (7) populations, as well as five populations for which the type was not recorded. There are 99 catarrhine primate networks, 13 platyrrhine networks, and 2 strepsirrhine networks. Sampling of the different contrasts represented in the ASNR is thus somewhat unbalanced but reflects the sampling effort present in the literature.

To test our hypothesis we require that, to the best extent possible, the edges represent prosocial contacts between individuals. Other contact types, such as dominance or mating, may reflect motives that are not relevant to the spread of cooperative behaviors, and proximity-based networks may reflect individuals who are co-located by chance or interest in a common resource rather than for social interaction. We therefore used the ASNR networks with the interaction types labeled "grooming", "physical contact", and "overall mix"; the "overall mix" category captures one additional network that recorded grooming behavior. We thus obtained 67 possible networks, which we regarded as undirected weighted networks.

Thirteen out of the 67 networks yielded negative $(b/c)^*$ values, which imply that spiteful behav-

Species	$(b/c)^*$	Neocortex Ratio	Brain mass	\overline{N}	$\langle k \rangle$	$\langle s \rangle$	C	$\tilde{C}_{ m w}$
Sapajus apella	12.59	2.25	66.63	12	7.17	7.17	0.69	0.08
Macaca arctoides	18.63	2.43	100.7	20	10.62	17.13	0.62	0.08
Cercopithecus campbelli	34.46	2.21	57.39	15	7.87	7.87	0.66	0.05
Papio cynocephalus	4.30	2.68	163.19	11	2.56	3.56	0.16	0.07
Macaca fascicularis	2.18	2.6	63.98	10.5	3.86	5.89	0.35	0.02
Macaca fuscata	12.98	2.45	102.92	9	6.52	92.53	0.91	0.06
Ateles geoffroyi	10.02	2.35	105.09	15	6	6	0.53	0.09
Colobus guereza	8.76	2.32	74.39	8	4.5	4.5	0.59	0.10
Ateles hybridus	11.81	2.35	103.05	17	8.47	794.47	0.81	0.09
Macaca mulatta	8.10	2.6	88.98	78	14.3	41.33	0.29	0.02
Pan paniscus	5.04	3.22	341.29	19	5.79	5.79	0.46	0.06
Papio papio	4.88	2.76	163.19	25	7.76	7.76	0.41	0.03
Erythrocebus patas	8.13	2.96	97.73	19	5.16	5.16	0.56	0.07
Macaca radiata	28.22	2.28	74.87	18	9.86	15.74	0.70	0.11
Macaca sylvanus	3.08	2.37	93.2	8	7	26.97	1	0.02
Macaca tonkeana	24.12	2.6	93.7	25	14.48	14.48	0.62	0.07
Pan troglodytes	11.42	3.22	368.35	24	8.58	8.58	0.65	0.08

TABLE I. Properties of primate social networks returned by our selection procedures, sorted by $(b/c)^*$. Values are medians of all the networks for *Papio cynocephalus*, *Macaca fasicularis*, *M. fuscata*, *M. mulatta*, and *M. radiata*. NCR: neocortex ratio, N: number of nodes, $\langle k \rangle$: average node degree, $\langle s \rangle$: average node strength, C: clustering coefficient, \tilde{C}_w : weighted clustering coefficient.

ior evolves instead of cooperation [37, 48]. We discarded these networks because we are interested in 185 cooperation under social dilemma situations, and because the qualitatively different interpretation 186 of a unit change for $(b/c)^*$ values above and below zero (i.e., a unit change in the positive direc-187 tion below zero means that spite evolves more easily, whereas a similar change above zero means 188 that cooperation evolves less easily) violates regression modeling assumptions. Additionally, we 189 discarded one network that was composed of two disconnected dyads and used the remaining 53 190 connected networks for our analysis. Most species had a single network in the repository. The 191 exceptions were Papio cynocephalus (which had 23 networks), Macaca fascicularis (2), M. fuscata 192 (4), M. mulatta (9), and M. radiata (2). For these species we took the median for $(b/c)^*$ and for 193 the network-based explanatory variables explained in Section II C to prevent a few species, such 194 as P. cynocephalus and M. mulatta, from dominating the set of networks to be analyzed. In this 195 manner, we reduced the 53 networks to observations on 17 species for further analysis (Table I). 196 We used the species-level neocortex ratio (NCR) estimate from [4] for all but one species, 197

Colobus guereza; a species-level NCR estimate was not available in [4], so we used the genus-level

198

NCR estimate from [3]. Additionally, we used the brain mass data from [49] for all species except 199 Papio papio, for which the data is not present. For Papio papio, we used the data of the closely 200 related species P. cynocephalus [50]. Because the size of several regions of the brain may correlate 201 with social complexity [5–7], we included overall brain mass as a relatively simple measure, when 202 compared to the NCR, of species' neurological complexity [8] that may also correlate with sociality 203 [51]. These two measures (i.e., brain mass and NCR) are highly correlated with each other (see 204 Section III). Given the unbalanced sampling mentioned above, we did not include controls for 205 phylogeny, social system, foraging behavior, whether the group was free-ranging or captive, or 206 type of behavior captured by the network. See Section IV for further discussion of this limitation. 207

C. Analysis

208

227

228

229

Data analysis was conducted in R [52]; the code is available at https://github.com/ngmaclaren/cooperationthreshold. We used the "MuMIn" package [53] to implement the model selection procedure
described below.

We fitted generalized linear models (GLMs) to test whether NCR and other variables were 212 associated with the difficulty of cooperation, $(b/c)^*$, which we used as the dependent variable. 213 We considered seven explanatory variables: NCR, brain mass in grams, and five network indices. 214 The five network indices are the number of nodes in the network, denoted by N, the average 215 degree over the N nodes, $\langle k \rangle$, the average node strength (i.e., the average of the weighted degree 216 over the N nodes), $\langle s \rangle$, the clustering coefficient, C, and the weighted clustering coefficient, $C_{\rm w}$. 217 The clustering coefficient is the average over all nodes of the local clustering coefficient; the local 218 clustering coefficient for the ith node is the number of triangles (i.e., (i, i'), (i, i''), and (i', i'')219 are edges of the network) divided by the number of possible triangles involving the ith node 220 (i.e., $k_i(k_i-1)/2$, where k_i is the node i's degree) [54, 55]. The weighted clustering coefficient is 221 calculated similarly to the unweighted version except that it uses the geometric mean of the edge 222 weights instead of a count of edges [56]. We include these network indices because each of these 223 indices can affect $(b/c)^*$ regardless of the potential relationship between brain size and $(b/c)^*$ [37]. 224 Because brain mass, body mass, $\langle s \rangle$, and $\tilde{C}_{\rm w}$ are positive and obey right-skewed distributions, we 225 used the natural logarithm transform of each of these variables. 226

We began our modeling process from a position of relative ignorance, including these seven explanatory variables as predictors. By design, our outcome variable, $(b/c)^*$, is positive and continuous, suggesting a model with gamma-distributed errors. To test our choice, we built five different

models, each with all seven explanatory variables, with different error models and link functions 230 (i.e., gamma and Gaussian distributions with both inverse and log links, and a quasi-Poisson model) 231 and calculated the deviances of each [57]. As expected, the gamma models fit well (χ^2 test with 232 d.f. = 8; p = 0.968 and 0.991 for the inverse and log links, respectively), whereas the other models 233 did not $(p \le 0.001 \text{ for each})$. The residual deviances associated with both gamma-based models 234 are small (inverse link: 2.90, log link: 2.01) relative to the remaining models (quasi-Poisson: 27.61, 235 Gaussian inverse link: 236.09, Gaussian log link: 374.50), further suggesting good fit [57]. Because 236 the model with gamma-distributed errors and the log link had the minimum residual deviance, we 237 used that model for further analysis [57]. 238

The number of explanatory variables (i.e., seven) is relatively large given the number of observa-239 tions (i.e., 17). Therefore, we ran an AIC-based model selection, as follows. First, we evaluated all 240 possible models—excluding any model with both brain mass and NCR as predictor variables—and 241 calculated the AICc for each model. AICc is a modification of the Akaike Information Criterion 242 (AIC) that is preferred for model selection when data sets are relatively small [58]. Specifically, 243 AICc is defined as AIC+ $(2k^2+2k)/(n-k-1)$, where k is the degrees of freedom of the model and 244 n is the number of observations. When n is small, AICc values increase more with each additional 245 model parameter than the traditional AIC does; the difference between the two metrics becomes 246 small when n is large. Model selection based on AICc thus tends to support fewer model param-247 eters at small n than traditional AIC. A recommended rule is to use AICc when n/k < 40 [58]; 248 for a model in this study with three predictor variables, an intercept, and an error parameter, we 249 obtain $n/k = 17/5 = 3.4 \ll 40$. We sorted all evaluated models by AICc: the models with minimal 250 AICc values realize the best fit to the data with the fewest variables.

III. RESULTS

252

We show the sorted AICc values for all 96 models which met our initial selection criteria in 253 Fig. 2. Figure 2 shows that the best and second-best models are fairly similar in terms of AICc, 254 but the third-best model has somewhat poorer AICc. Setting a cutoff at Δ AICc = 3, where Δ AICc 255 means the absolute difference in the AICc value relative to the smallest value, allows us to focus 256 on two models that are similar in terms of AICc but clearly better than any other alternatives. 257 We summarize these two models in Table II. These two models are superior to the full model 258 in terms of AICc (full model AICc: 132.39, Model 1: 106.91, Model 2: 108.01) and collinearity 250 (maximum variance inflation factor for the full model: 5.08, Model 1: 1.03, Model 2: 1.02) without 260

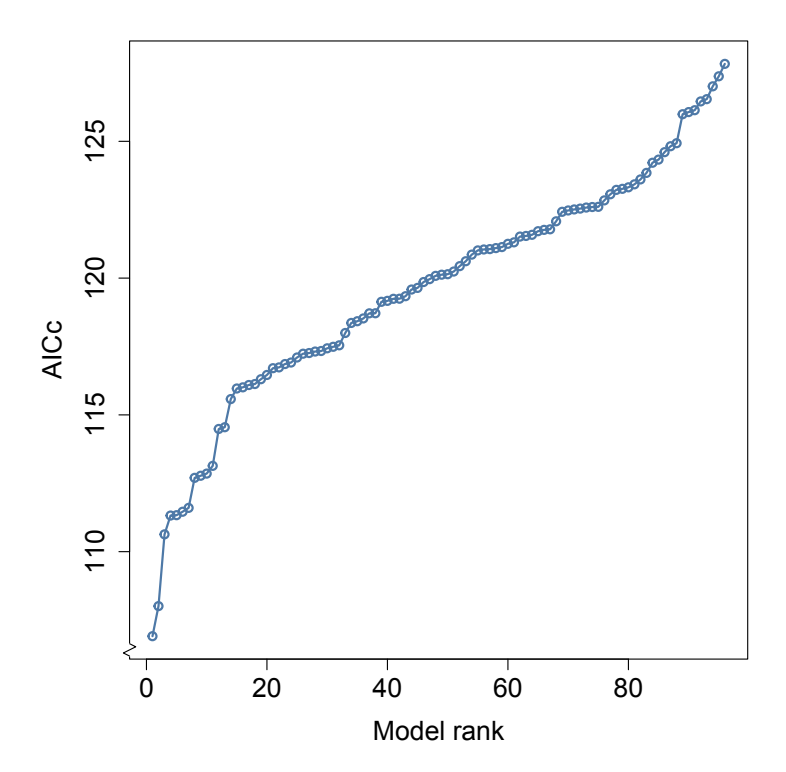


FIG. 2. Akaike Information Criterion adjusted for small samples (AICc) for all possible models. Possible models are generalized linear models with gamma-distributed errors, a natural logarithm link function, and zero or more of the following explanatory variables: neocortex ratio, brain size, number of nodes, average node degree, average node strength, clustering coefficient, and weighted clustering coefficient.

a substantial reduction in variance explained (full model McFadden's pseudo- R^2 : 0.77, Model 1: 0.73, Model 2: 0.72).

The two best models both include a measure of brain size—overall brain mass in Model 1 and 263 NCR in Model 2—and two network features: average node degree $\langle k \rangle$ and the weighted clustering 264 coefficient $\tilde{C}_{\rm w}$ (Table II). As is expected given the correlation between brain mass and NCR in 265 this data (r = 0.843, mentioned above), coefficient estimates for the two models are similar: the 266 coefficients on both brain size variables are both negative, whereas the coefficients on average node 267 degree and weighted clustering are positive. Thus, we find that, when average degree and weighted 268 clustering are held constant, brain size is inversely associated with $(b/c)^*$ in this data: primates 269 with larger brains are associated with social networks that favor the spread of cooperation. We 270 visualize the association between NCR and $(b/c)^*$, controlling for average degree and weighted 271 clustering, in Fig. 3. 272

Although overall trends in the data support the social brain hypothesis, there is substantial uncertainty in the coefficient estimates (see Table II). We visualize this uncertainty in Fig. 4, which

273

274

			95% CI			
Model 1	Estimate	SE	Lower	Upper		
Intercept	6.398	1.503	3.469	9.277		
Brain mass	-0.522	0.256	-0.958	-0.051		
$\langle k angle$	0.138	0.041	0.050	0.230		
$ ilde{C}_{ m w}$	0.944	0.243	0.390	1.460		
AICc	106.910					
Deviance	2.353					
Pseudo- \mathbb{R}^2	0.73					
			95% CI			
Model 2	Estimate	SE	Lower	Upper		
Intercept	5.809	1.329	3.134	8.479		
Neocortex ratio	-0.827	0.437	-1.590	-0.010		
$\langle k angle$	0.135	0.042	0.048	0.228		
$ ilde{C}_{ m w}$	0.844	0.249	0.281	1.361		
AICc	108.010					
Deviance	2.507					
Pseudo- R^2	0.72					

TABLE II. The best two models, i.e., the models with $\Delta \text{AICc} < 3$. The dependent variable is $(b/c)^*$. All models are generalized linear models with gamma-distributed errors and a natural logarithm link. A negative coefficient indicates that a larger value of the predictor is associated with a smaller value of $(b/c)^*$, suggesting that cooperation spreads more easily on a network. SE stands for the standard error; CI stands for confidence interval; $\langle k \rangle$ and $\tilde{C}_{\rm w}$ represent average degree and the weighted clustering coefficient, respectively.

shows the point estimate for each coefficient (open markers) in both models (indicated by color and marker shape) along with the profile likelihood 95% confidence intervals (horizontal lines). The confidence intervals are all relatively wide compared with the magnitude of the coefficient, suggesting that the size and noisiness of our data inhibit our ability to make precise estimates of the relationship between brain size and $(b/c)^*$.

280

281

282

283

284

285

287

Finally, we note that neither of the best two models has more than three explanatory variables, suggesting that adding more explanatory variables would not be useful in better explaining $(b/c)^*$ across the different networks. This observation indicates that our data do not support differentiating between the effects of brain mass and neocortex ratio by, for example, including one as a control on the other in a regression model. The failure of group size N to appear in the best models is also notable, which we discuss in the Discussion section. This finding suggests that the relationship between brain size and the spread of cooperative behavior may be independent of group size. Finally, neither the average weighted degree $\langle s \rangle$ nor the unweighted clustering coefficient C

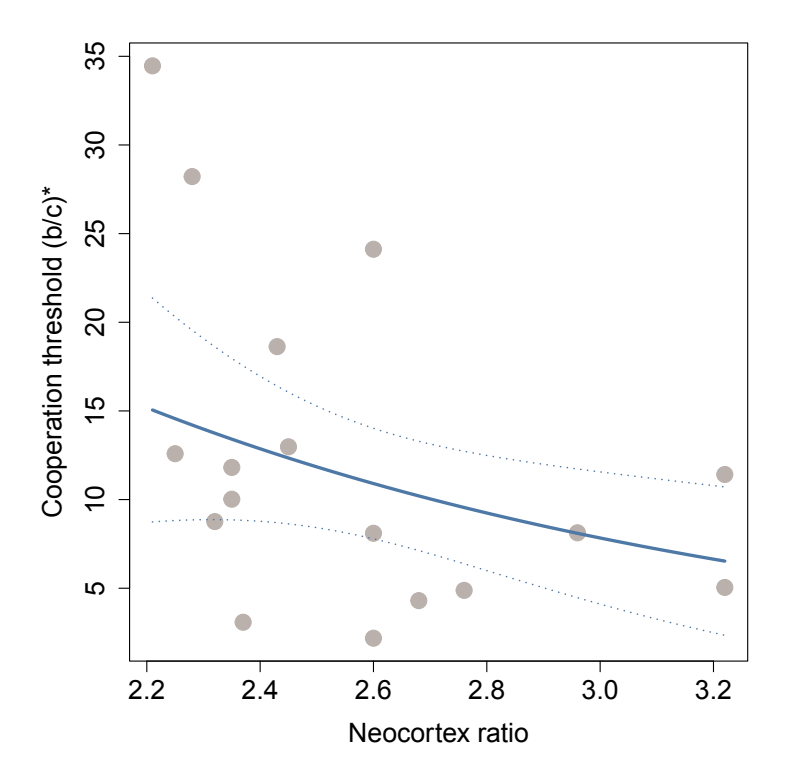


FIG. 3. Threshold for cooperation, $(b/c)^*$, as a function of the neocortex ratio. Each circle represents a primate species. The solid line represents the predicted $(b/c)^*$ given median values for average degree and weighted clustering coefficient. The dotted lines indicate twice the standard error of prediction.

288 appeared in the five best models.

IV. DISCUSSION

Our findings suggest that primate species with larger brains tend to form networks which, based on results from game theory [37], support the spread of cooperative behaviors. Thus, our primary results are consistent with the social brain hypothesis. Our results are also consistent with previous findings on the effect of network structure on cooperation in primates [59].

Group size and NCR are only weakly correlated with each other in our data (r = 0.203). This result is only marginally consistent with previous studies, which showed a strong association between group size, which has been used as a proxy for social complexity [11], and NCR; this association is a central result supporting the social brain hypothesis [60]. A weak association between group size and NCR in our data may be due to different definitions of the group size used in our study and the previous ones. The group size used in this study is the observed number of individuals in a single group. That group was captive in some studies, and there may be other

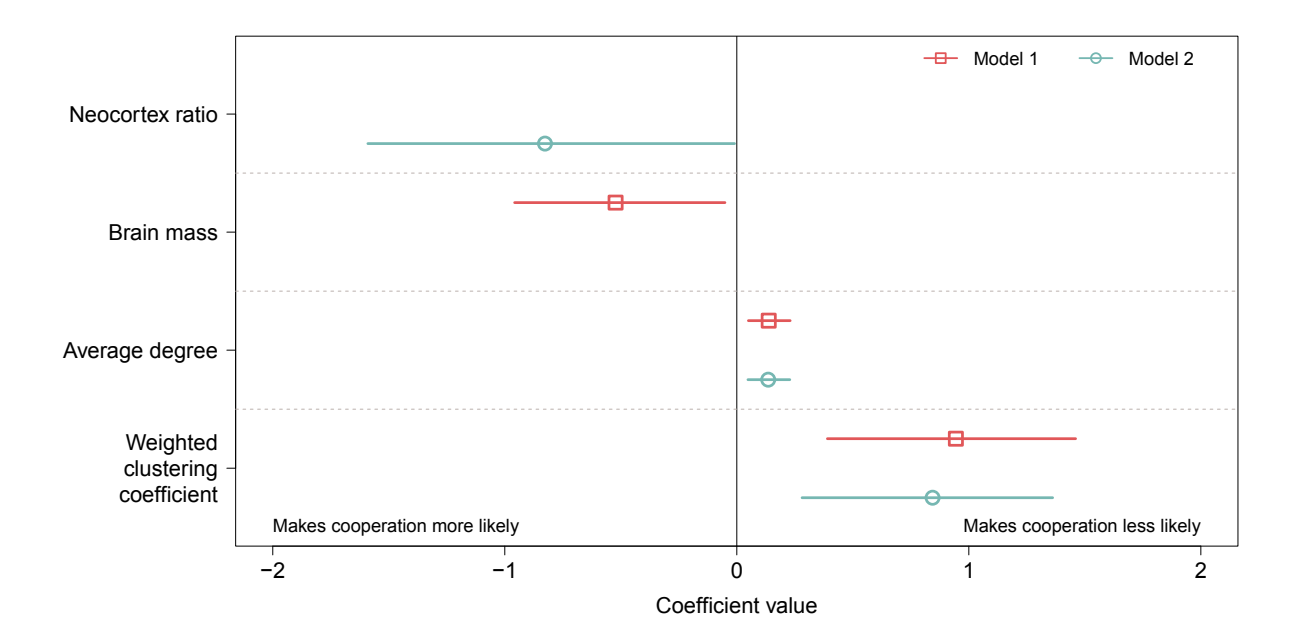


FIG. 4. Coefficient estimates for the two models with $\Delta \text{AICc} < 3$. Both models are generalized linear models with gamma-distributed errors and a natural logarithm link function and express the association between three explanatory variables and $(b/c)^*$. Each model is represented by a different color and type of marker. The markers represent the coefficient values. The lines represent the profile likelihood 95% confidence intervals.

constraints on the observed group size in a particular study that may make the group size value different from what may be typical in wild populations. This difference may have depressed the relationship between group size and the NCR, and also the relationship between group size and cooperation in the present study. Alternatively, we note that primate groups may form for a variety of reasons, such as protection from predators, which neither relate specifically to cooperation nor necessarily indicate an increased cognitive demand on group members. By including group size as a potential predictor of the cooperation threshold, we hypothesized that groups with larger size will have consistent differences in their cooperation threshold from groups of smaller size. We found that this is not the case within the limits of our analysis. Thus, our present findings are orthogonal to previous tests of the social brain hypothesis.

Our data indicate a notable level of uncertainty in the observed trends. An important reason for this uncertainty is the relatively small sample size of our final data set. Additionally, as we described in Section II, our models do not control for a variety of factors, such as phylogeny and study design. Omitting these variables might account for some of our reported error variance. However, these factors are represented in a very uneven way in the primate networks available

in the ASNR, limiting our ability to control for them in our models in a meaningful way. For 316 example, of the 17 species in our final data set, 11 are cercopithecine primates and of those, seven 317 are macaques. No lemur or other strepsirrhine species are represented at all. The situation is 318 even more extreme in the data set prior to aggregation to the species level, in which 44 of the 53 319 networks came from two cercopithecine genera: Papio (23) and Macaca (21). Thus, although the 320 phylogenetic signal in group size and related variables has been previously shown to be relatively 321 weak [61], we are limited in our ability to control for phylogenetic effects that may be present in 322 our model. We face a similar situation in attempting to control for study design, which can affect 323 the structure of observed networks [62]: in our data, most groups were sampled according to social 324 group membership, none were sampled according to a geographic area, and the only captive groups 325 were 10 of the 21 macaque networks. Finally, some uncertainty in our estimates may be due to the 326 brain mass and NCR measurements themselves, which are difficult to obtain and thus not based on large samples of individuals nor available for all species [63]. Because of these conditions, we have 328 chosen to simplify our model to accommodate a small sample [64], rather than take a maximal 329 approach, with which we would include as many theoretically important variables in the model as 330 possible [65, 66]. We recognize that our decisions reduce both the sample size and the potential 331 generalizability of our study [67]. Additional data from species more evenly spread across primate 332 taxa will help address these concerns, as well as support mediation analysis to better test between 333 competing causal hypotheses. 334

From a theoretical perspective, our work is also limited by the assumptions made by Allen et al.'s theory [37]. Specifically, their theory assumes fixed, undirected networks and binary strategies (i.e., cooperation or defection). Such assumptions do not realistically represent primate social networks, which may be dynamic, have asymmetric ties (i.e., individual A grooms individual B more than the reverse), and be characterized by complex behavioral strategies. This lack of an explicit connection between models and reality has been recognized as a major challenge in evolutionary game theory [68]. The strength of Allen et al.'s results and others is in providing insight into the general mechanisms of the evolution of cooperation [69]. Our study addresses this gap by showing that predictions from the social brain hypothesis, based on observations, are in line with those from evolutionary game theory.

335

336

337

338

339

341

342

343

344

345

346

Despite these caveats, the present results allow us to make several additional observations. For example, we observe that cooperation spreads less easily on networks in which individuals tend to have many social partners (i.e., large average degree) or tend to form clusters (i.e., connected triangles). While the former observation agrees with the literature [36, 37], the latter is apparently

inconsistent with the concept of spatial reciprocity, which states that high clustering in networks promotes cooperation [29, 40, 41]. In fact, results supporting spatial reciprocity have been derived for the fraction of cooperators in the quasi-stationary state of evolutionary dynamics in relatively large networks rather than the fixation probability for the cooperator strategy; we examined the latter quantity in this study. The effect of clustering on the fixation probability for cooperation is not systematically known. For example, some numerical simulations suggest that clustering, which is present in most empirical networks, does not facilitate the fixation of cooperation [36, 70]. Therefore, our results are in fact not contradictory to the known results for spatial reciprocity, and fixation of cooperation in clustered networks remains to be investigated.

Cooperative group living is often advantageous in the animal kingdom because it can provide protection from predators and increase the efficiency of foraging tactics [20, 71]. However, one of the most commonly cited disadvantages to cooperative group living is the increase in disease transmission potential [71, 72]. In fact, previous work suggests that the average degree is the most important aspect of network structure in determining the transmission potential for pathogens on a network [62]. Our results show that average degree is negatively associated with the evolution of cooperation, a finding supported by previous theoretical work [36]. Given that small average degrees are beneficial for both enhancing cooperation and reducing pathogen transmission opportunity, cooperation and protection against disease transmission potential might have coevolved through a decrease in the average degree of social networks. Maintaining contacts is also costly for individuals. However, a large average degree helps robustness of networks against node and edge failures [17, 73]. We may be able to further discussion of the evolution of network structure and social brain hypotheses by simultaneously taking into account multiple functions of animal society such as cooperation, protection against infection, robustness, and communication efficiency.

The present work also opens avenues for further work to explore the intersection between the social brain hypothesis, networks, and cooperation. For example, most of the social networks in our sample are grooming networks. However, network structure may vary according to the type of prosocial contact even for the same species of animals [62]. It is not currently known if differences in network structure associated with different behaviors also reflect differences in the spread of cooperation or other indices of social complexity. Furthermore, the spread of spite on ostensibly prosocial networks is an important possibility, but insufficiently characterized. Although further comparative work along these lines is currently limited by available data [46], various technological and algorithmic developments of automatic data collection [17, 74] are expected to allow us to access more data and explore these topics in the near future.

ACKNOWLEDGMENTS

N. Masuda acknowledges support from AFOSR European Office (under Grant No. FA9550-19-1-7024), the Japan Science and Technology Agency (JST) Moonshot R&D (under Grant No. JPMJMS2021), the National Science Foundation (under Grant Nos. 2052720 and 2204936), and JSPS KAKENHI (under Grant Nos. JP 21H04595 and 23H03414). M. Collier acknowledges funding from the Morris Animal Foundation (under Grant No. D22ZO-059). We thank Shweta Bansal for her thoughtful comments on this work. We thank Pratha Sah, Jose Mendez, Grant Rosensteel, Elly Meng, and Sania Ali for their contributions to the development and growth of the Animal Social Network Repository.

AUTHOR CONTRIBUTIONS

N.M. designed the study. L.M. and N.G.M. analyzed the data, supervised by N.M. M.C. curated the data. N.M. and N.G.M. wrote the manuscript with contributions by L.M. and M.C. All authors reviewed and approved the manuscript.

DATA AVAILABILITY

The data for this study comes from the Animal Social Network Repository, Version 2, located at https://github.com/bansallab/asnr (DOI: 10.5281/zenodo.7595404) [46, 47].

COMPETING INTERESTS

The authors declare no competing interests.

382

391

395

398

399

400

REFERENCES

- [1] R. I. M. Dunbar. The social brain hypothesis. Evolutionary Anthropology: Issues, News, and Reviews, 6(5):178–190, 1998.
- [2] P. M. Kappeler, T. Clutton-Brock, S. Shultz, and D. Lukas. Social complexity: patterns, processes,
 and evolution. Behavioral Ecology and Sociobiology, 73:5, 2019.
- [3] R. I. M. Dunbar. Neocortex size as a constraint on group size in primates. *Journal of Human Evolution*, 22(6):469–493, 1992.

- [4] H. Kudo and R. I. M. Dunbar. Neocortex size and social network size in primates. *Animal Behaviour*, 62(4):711–722, 2001.
- [5] K. C. Bickart, C. I. Wright, R. J. Dautoff, B. C. Dickerson, and L. F. Barrett. Amygdala volume and social network size in humans. *Nature Neuroscience*, 14(2):163–164, 2011.
- [6] R. Kanai, B. Bahrami, R. Roylance, and G. Rees. Online social network size is reflected in human brain structure. *Proceedings of the Royal Society B: Biological Sciences*, 279(1732):1327–1334, 2012.
- [7] P. A. Lewis, R. Rezaie, R. Brown, N. Roberts, and R. I. M. Dunbar. Ventromedial prefrontal volume predicts understanding of others and social network size. *NeuroImage*, 57(4):1624–1629, 2011.
- [8] A. R. DeCasien, S. A. Williams, and J. P. Higham. Primate brain size is predicted by diet but not sociality. *Nature Ecology & Evolution*, 1(5):0112, 2017.
- [9] S. E. Street, A. F. Navarrete, S. M. Reader, and K. N. Laland. Coevolution of cultural intelligence, extended life history, sociality, and brain size in primates. *Proceedings of the National Academy of Sciences*, 114(30):7908–7914, 2017.
- [10] L. E. Powell, K. Isler, and R. A. Barton. Re-evaluating the link between brain size and behavioural ecology in primates. *Proceedings of the Royal Society B: Biological Sciences*, 284(1865):20171765, 2017.
- [11] R. I. M. Dunbar and S. Shultz. Why are there so many explanations for primate brain evolution?

 Philosophical Transactions of the Royal Society B: Biological Sciences, 372(1727):20160244, 2017.
- [12] S. Shultz and R. I. M. Dunbar. Socioecological complexity in primate groups and its cognitive correlates.

 Philosophical Transactions of the Royal Society B, 377(1860):20210296, 2022.
- ⁴²⁶ [13] J. Lehmann and R. I. M. Dunbar. Network cohesion, group size and neocortex size in female-bonded old world primates. *Proceedings of the Royal Society B: Biological Sciences*, 276(1677):4417–4422, 2009.
- 142 [14] C. Pasquaretta, M. Levé, N. Claidiere, E. Van de Waal, A. Whiten, A. J. J. MacIntosh, M. Pelé, M. L.
- Bergstrom, C. Borgeaud, S. F. Brosnan, M. C. Crofoot, L. M. Fedigan, C. Fichtel, L. M. Hopper, M. C.
- Mareno, O. Petit, A. V. Schnoell, E. Polizzi di Sorrentino, B. Theirry, B. Tiddi, and C. Sueur. Social
- networks in primates: smart and tolerant species have more efficient networks. Scientific Reports, 4(1):
- 7600, 2014.
- [15] N. Pinter-Wollman, E. A. Hobson, J. E. Smith, A. J. Edelman, D. Shizuka, S. De Silva, J. S. Waters,
 S. D. Prager, T. Sasaki, G. Wittemyer, J. Fewell, and D. B. McDonald. The dynamics of animal social
 networks: analytical, conceptual, and theoretical advances. *Behavioral Ecology*, 25(2):242–255, 2014.
- [16] J. Kruase, R. James, D. W. Franks, and D. P. Croft, editors. Animal Social Networks. Oxford University
 Press, Oxford, UK, 2015.
- 438 [17] J. B. Brask, S. Ellis, and D. P. Croft. Animal social networks: an introduction for complex systems
 439 scientists. *Journal of Complex Networks*, 9(2):cnab001, 2021.
- [18] S. Bansal, B. T. Grenfell, and L. A. Meyers. When individual behaviour matters: homogeneous and network models in epidemiology. *Journal of the Royal Society Interface*, 4(16):879–891, 2007.
- 442 [19] J. M. Smith. Evolution and the Theory of Games. Cambridge University Press, 1982.

- [20] P. M. Kappeler and C. P. Van Schaik. *Cooperation in Primates and Humans*. Springer, Berlin, Germany, 2006.
- [21] R. Noë. Cooperation experiments: coordination through communication versus acting apart together.

 Animal Behaviour, 71(1):1–18, 2006.
- ⁴⁴⁷ [22] D. L. Cheney. Extent and limits of cooperation in animals. *Proceedings of the National Academy of Sciences of the United States of America*, 108(supplement_2):10902-10909, 2011.
- [23] D. P. Croft, M. Edenbrow, and S. K. Darden. Assortment in social networks and the evolution of cooperation. In *Animal Social Networks*, pages 13–23. Oxford University Press, Oxford, UK, 2015.
- [24] K. McAuliffe and A. Thornton. The psychology of cooperation in animals: an ecological approach.
 Journal of Zoology, 295(1):23-35, 2015.
- ⁴⁵³ [25] S. Gokcekus, E. F. Cole, B. C. Sheldon, and J. A. Firth. Exploring the causes and consequences of cooperative behaviour in wild animal populations using a social network approach. *Biological Reviews*, 96(5):2355–2372, 2021.
- 456 [26] T. Clutton-Brock. Cooperation between non-kin in animal societies. Nature, 462(7269):51–57, 2009.
- [27] D. L. Cheney, L. R. Moscovice, M. Heesen, R. Mundry, and R. M. Seyfarth. Contingent cooperation
 between wild female baboons. Proceedings of the National Academy of Sciences of the United States of
 America, 107(21):9562–9566, 2010.
- ⁴⁶⁰ [28] D. Fudenberg and D. K. Levine. *The Theory of Learning in Games*. MIT Press, Cambridge, MA, 1998.
- 461 [29] M. A. Nowak. Five rules for the evolution of cooperation. Science, 314:1560–1563, 2006.
- [30] E. A. Smith. Communication and collective action: language and the evolution of human cooperation.

 Evolution and Human Behavior, 31(4):231–245, 2010.
- 464 [31] M. Salahshour. Coevolution of cooperation and language. Physical Review E, 102(4):042409, 2020.
- 465 [32] G. Szabó and G. Fáth. Evolutionary games on graphs. Physics Reports, 446:97–216, 2007.
- [33] M. Perc, J. Gómez-Gardeñes, A. Szolnoki, L. M. Floría, and Y. Moreno. Evolutionary dynamics of
 group interactions on structured populations: a review. Journal of the Royal Society Interface, 10(80):
 20120997, 2013.
- [34] M. Perc, J. J. Jordan, D. G. Rand, Z. Wang, S. Boccaletti, and A. Szolnoki. Statistical physics of human cooperation. *Physics Reports*, 687:1–51, 2017.
- [35] K. Takács, J. Gross, M. Testori, S. Letina, A. R. Kenny, E. A. Power, and R. P. M. Wittek. Networks
 of reliable reputations and cooperation: a review. *Philosophical Transactions of the Royal Society B:* Biological Sciences, 376(1838):20200297, 2021.
- 474 [36] H. Ohtsuki, Ch. Hauert, E. Lieberman, and M. A. Nowak. A simple rule for the evolution of cooperation 475 on graphs and social networks. *Nature*, 441(7092):502–505, 2006.
- 476 [37] B. Allen, G. Lippner, Y.-T. Chen, B. Fotouhi, N. Momeni, S.-T. Yau, and M. A. Nowak. Evolutionary dynamics on any population structure. *Nature*, 544(7649):227–230, 2017.
- [38] F. C. Santos and J. M. Pacheco. Scale-free networks provide a unifying framework for the emergence of cooperation. *Physical Review Letters*, 95(9):098104, 2005.

- [39] F. C. Santos, J. M. Pacheco, and T. Lenaerts. Evolutionary dynamics of social dilemmas in structured
 heterogeneous populations. Proceedings of the National Academy of Sciences of the United States of
 America, 103(9):3490-3494, 2006.
- 483 [40] M. A. Nowak and R. M. May. Evolutionary games and spatial chaos. *Nature*, 359(6398):826–829, 1992.
- [41] Ch. Hauert. Fundamental clusters in spatial 2 × 2 games. Proceedings of the Royal Society B: Biological
 Sciences, 268(1468):761–769, 2001.
- [42] D. Aldous and J. A. Fill. Reversible markov chains and random walks on graphs, 2002. Unfinished
 monograph, recompiled 2014 (2002) available at
- http://www.stat.berkeley.edu/~aldous/RWG/book.html. Accessed on August 6, 2022.
- [43] N. Masuda, M. A. Porter, and R. Lambiotte. Random walks and diffusion on networks. *Physics Reports*, 716:1–58, 2017.
- [44] M. A. Nowak, A. Sasaki, C. Taylor, and D. Fudenberg. Emergence of cooperation and evolutionary
 stability in finite populations. *Nature*, 428(6983):646–650, 2004.
- [45] M. A. Nowak. Evolutionary Dynamics. Belknap Press of Harvard University Press, Cambridge, MA,
 2006.
- [46] P. Sah, J. D. Méndez, and S. Bansal. A multi-species repository of social networks. Scientific Data, 6:
 44, 2019.
- [47] M. Collier, S. Ali, and S. Bansal. Animal social network repository, August 2021. URL https: //doi.org/10.5281/zenodo.7595404. Accessed Oct 31, 2022.
- [48] Q. Su, A. McAvoy, and J. B. Plotkin. Evolution of cooperation with contextualized behavior. Science
 Advances, 8(6):eabm6066, 2022.
- 501 [49] J. B. Smaers, R. S. Rothman, D. R. Hudson, A. M. Balanoff, B. Beatty, D. K. N. Dechmann, D. de Vries,
- J. C. Dunn, J. G. Fleagle, C. C. Gilbert, A. Goswami, A. N. Iwaniuk, W. L. Jungers, M. Kerney, D. T.
- Ksepka, P. R. Manger, C. S. Mongle, F. J. Rohlf, N. A. Smith, C. Soligo, V. Weisbecker, and K. Safi.
- The evolution of mammalian brain size. Science Advances, 7(18):eabe2101, 2021.
- [50] T. K. Newman, C. J. Jolly, and J. Rogers. Mitochondrial phylogeny and systematics of baboons
 (Papio). American Journal of Physical Anthropology, 124(1):17–27, 2004.
- J. B. Smaers, C. S. Mongle, K. Safi, and D. K. N. Dechmann. Allometry, evolution and development
 of neocortex size in mammals. Progress in Brain Research, 250:83–107, 2019.
- [52] R Core Team. R: A Language and Environment for Statistical Computing. R Foundation for Statistical Computing, Vienna, Austria, 2022. URL https://www.R-project.org/.
- [53] K. Bartoń. MuMIn: Multi-Model Inference, 2022. URL https://CRAN.R-project.org/package=
 MuMIn. R package version 1.47.1.
- [54] S. Wasserman and K. Faust. Social Network Analysis: Methods and Applications. Cambridge University
 Press, New York, NY, 1994.
- 515 [55] M. Newman. Networks. Oxford University Press, Oxford, UK, 2nd edition, 2018.
- 516 [56] G. Fagiolo. Clustering in complex directed networks. Physical Review E, 76(2):026107, 2007.

- [57] J. J. Faraway. Extending the Linear Model with R: Generalized Linear, Mixed Effects and Nonparametric
 Regression Models. Chapman and Hall/CRC, Boca Raton, FL, 2nd edition, 2016.
- [58] K. P. Burnham and D. R. Anderson. Model Selection and Multi-Model Inference. Springer-Verlag, New
 York, NY, 2nd edition, 2002.
- [59] B. Voelkl and C. Kasper. Social structure of primate interaction networks facilitates the emergence of cooperation. *Biology Letters*, 5(4):462–464, 2009.
- [60] R. I. M. Dunbar and S. Shultz. Social complexity and the fractal structure of group size in primate social evolution. *Biological Reviews*, 96(5):1889–1906, 2021.
- [61] J. M. Kamilar and N. Cooper. Phylogenetic signal in primate behaviour, ecology and life history.
 Philosophical Transactions of the Royal Society B: Biological Sciences, 368(1618):20120341, 2013.
- [62] M. Collier, G. F. Albery, G. C. McDonald, and S. Bansal. Pathogen transmission modes determine
 contact network structure, altering other pathogen characteristics. *Proceedings of the Royal Society B:* Biological Sciences, 289(1989):20221389, 2022.
- [63] H. Stephan, H. Frahm, and G. Baron. New and revised data on volumes of brain structures in insectivores and primates. *Folia Primatologica*, 35(1):1–29, 1981.
- [64] H. Matuschek, R. Kliegl, S. Vasishth, H. Baayen, and D. Bates. Balancing type i error and power in
 linear mixed models. *Journal of Memory and Language*, 94:305–315, 2017.
- [65] D. J. Barr, R. Levy, C. Scheepers, and H. J. Tily. Random effects structure for confirmatory hypothesis
 testing: Keep it maximal. *Journal of Memory and Language*, 68(3):255–278, 2013.
- 536 [66] R. McElreath. Statistical rethinking: A Bayesian course with examples in R and Stan. Chapman and 537 Hall/CRC, 2016.
- 538 [67] T. Yarkoni. The generalizability crisis. Behavioral and Brain Sciences, 45:1–78, 2022.
- [68] M. Jusup, P. Holme, K. Kanazawa, M. Takayasu, I. Romić, Z. Wang, S. Geček, T. Lipić, B. Podobnik,
 L. Wang, W. Luo, T. Klanjšček, J. Fan, and S. Boccaletti. Social physics. *Physics Reports*, 948:1–148,
 2022.
- ⁵⁴² [69] E. Akçay. Deconstructing evolutionary game theory: coevolution of social behaviors with their evolutionary setting. *The American Naturalist*, 195(2):315–330, 2020.
- 544 [70] Z.-X. Wu, Z. Rong, and H.-X. Yang. Community structure benefits the fixation of cooperation under 545 strong selection. arXiv preprint arXiv:1408.3267, 2014.
- [71] R. D. Alexander. The evolution of social behavior. Annual Review of Ecology and Systematics, 5:
 325–383, 1974.
- ⁵⁴⁸ [72] W. J. Freeland. Pathogens and the evolution of primate sociality. *Biotropica*, 8(1):12–24, 1976.
- [73] R. Cohen and S. Havlin. Complex Networks: Structure, Robustness and Function. Cambridge University
 Press, Cambridge, UK, 2010.
- ⁵⁵¹ [74] J. Krause, S. Krause, R. Arlinghaus, I. Psorakis, S. Roberts, and C. Rutz. Reality mining of animal social systems. *Trends in Ecology & Evolution*, 28(9):541–551, 2013.